bioRxiv preprint doi: https://doi.org/10.1101/452391; this version posted October 24, 2018. The copyright holder for this preprint (which was not certified by peer review) is the author/funder, who has granted bioRxiv a license to display the preprint in perpetuity. It is made available under aCC-BY 4.0 International license.

Dysregulation of circular RNAs in myotonic dystrophy type 1

Christine Voellenkle [1], Alessandra Perfetti [1], Matteo Carrara [1], Paola Fuschi [1], Laura Valentina Renna [2], Marialucia Longo [1], Rosanna Cardani [2], Rea Valaperta [3], Gabriella Silvestri [4], Ivano Legnini [5], Irene Bozzoni [5], Denis Furling [6], Carlo Gaetano [7], Germana Falcone [8], Giovanni Meola [2,9,10], Fabio Martelli [1*]

[1] Molecular Cardiology Laboratory, IRCCS Policlinico San Donato, San Donato Milanese, Milan, Italy.

[2] Laboratory of Muscle Histopathology and Molecular Biology, IRCCS Policlinico San Donato, San Donato Milanese, Milan, Italy.

[3] Research Laboratories, IRCCS Policlinico San Donato, San Donato Milanese, Milan, Italy

[4] Department of Geriatrics, Orthopaedic and Neuroscience, Institute of Neurology, Catholic University of Sacred Heart, Fondazione Policlinico Gemelli, Rome, Italy.

[5] Department of Biology and Biotechnology "Charles Darwin", Sapienza University of Rome, Italy.

[6] Sorbonne Université, INSERM, Association Institut de Myologie, Centre de Recherche en Myologie, F-75013 Paris, France.

[7] Laboratory of Epigenetics, Istituti Clinici Scientifici Maugeri, Pavia, Italy.

[8] Institute of Cell Biology and Neurobiology, National Research Council, Monterotondo, Rome, Italy.

[9] Department of Neurology, IRCCS Policlinico San Donato, San Donato Milanese, Milan, Italy.

[10] Department of Biomedical Sciences for Health, University of Milan, Milan, Italy.

bioRxiv preprint doi: https://doi.org/10.1101/452391; this version posted October 24, 2018. The copyright holder for this preprint (which was not certified by peer review) is the author/funder, who has granted bioRxiv a license to display the preprint in perpetuity. It is made available under aCC-BY 4.0 International license.

* Corresponding author: Fabio Martelli, PhD

Molecular Cardiology Laboratory, IRCCS Policlinico San Donato

Via Morandi, 30-20097, San Donato Milanese, Milan, Italy.

Phone: +390226437762

Email: fabio.martelli@grupposandonato.it

Short title:

Circular RNAs in DM1

Keywords:

Musculoskeletal system, Muscular dystrophies, alternative splicing, circular RNA

bioRxiv preprint doi: https://doi.org/10.1101/452391; this version posted October 24, 2018. The copyright holder for this preprint (which was not certified by peer review) is the author/funder, who has granted bioRxiv a license to display the preprint in perpetuity. It is made available under aCC-BY 4.0 International license.

Abstract

Circular RNAs (circRNAs) constitute a recently re-discovered class of non-coding RNAs functioning as sponge for miRNAs and proteins, affecting RNA splicing and regulating transcription. CircRNAs are generated by "back-splicing", linking covalently 3'- and 5'-ends of exons. Thus, circRNA levels might be deregulated in conditions associated to altered RNA-splicing. Indeed, increasing evidence indicates their role in human diseases. Specifically, myotonic dystrophy type 1 (DM1) is a multisystemic disorder caused by expanded CTG-repeats in the *DMPK* gene, resulting in abnormal mRNA-splicing. In this investigation, circRNAs expressed in DM1 skeletal muscles were identified by analyzing RNA-sequencing data-sets followed by qPCR validation. In muscle biopsies, out of 9 tested, 4 transcripts showed an increased circular fraction: CDYL, HIPK3, RTN4_03 and ZNF609. The circular fraction values correlated positively with skeletal muscle strength and Receiver-Operating-Characteristics curves showed that these four circRNAs allow to distinguish DM1 patients from controls. The identified circRNAs were also detectable in peripheral-blood-mononuclear-cells (PBMCs) and plasma of DM1 patients, but they were not regulated significantly, indicating a tissue-selectivity of the identified modulations. Finally, increased circular fractions of RTN4_03 and ZNF609 were also observed in differentiated myogenic cell lines derived from DM1 patients.

In conclusion, this proof-of-principle study identified circRNA dysregulation in DM1 patients.

Introduction

Myotonic dystrophy type 1 (DM1), also known as Steinert disease (OMIM #160900), is an autosomal dominant multi-systemic disorder, with a spectrum of clinical manifestations that include myotonia, reduced muscle strength, cardiac arrhythmia, insulin resistance, cataracts, hypogonadism, and, in the most severe forms, cognitive defects [1-4]. The genetic defect in DM1 results from the

bioRxiv preprint doi: https://doi.org/10.1101/452391; this version posted October 24, 2018. The copyright holder for this preprint (which was not certified by peer review) is the author/funder, who has granted bioRxiv a license to display the preprint in perpetuity. It is made available under aCC-BY 4.0 International license.

dynamic expansion of CTG repeats in the 3' untranslated region of the *dystrophia myotonica protein kinase* (*DMPK)* gene [5]. Severity of the disorder generally increases with the number of CTG repeats: healthy individuals have up to 40 repeats, patients with classic DM1 have 100-1000 repeats, and patients affected by congenital DM1 can have more than 2000 CTG repeats.

A major patho-mechanism underpinning DM1 is the generation of toxic RNAs containing expanded CUG triplets that accumulate as distinctive nuclear *foci* and dysregulate the activity of RNA processing factors, including MBNL1, CELF1, as well as Staufen1 and DDX5 [6-12]. Expanded CUG repeats have been demonstrated to be toxic *per se* in several cell types and animal models [13-15], disrupting pre-mRNA alternative splicing [16]. RNA splicing alterations result in the re-emergence of developmentally immature alternative splicing and polyadenylation patterns in adult muscles, as well as in alterations of localization and turnover of specific transcripts [7,16-19].

Circular RNAs (circRNAs) are covalently closed loop-structure RNAs. They are generated by splicing events occurring on maturing pre-mRNAs in a different order than their genomic sequence, joining together a donor site with an upstream acceptor site [20-23].

CircRNAs have no accessible 5′ or 3′ ends and are not poly-adenylated, escaping detection by many analytical and bioinformatics tools that are widely used in RNA biology. Indeed, for a long time, circRNAs were dismissed as rare aberrant by-products of the splicing process. More recently, large RNA deep-sequencing projects and the development of bioinformatics tools enabling the analysis of extensive data-sets, allowed the identification of significant proportions of back-splice junction reads associated to circRNAs in virtually all eukaryotic organisms [24-28]. While many circRNAs likely are byproducts of RNA splicing mechanisms, some circRNAs can be even more abundant than the linear counterparts [27] and specific biological functions have been associated to a rapidly increasing number of them. Certain circRNAs contain sequences complementary to the seed of a specific microRNA (miRNA), sequestering it and therefore reducing its bioavailability for target-mRNA inhibition [29]. A prototype of this is CDR1AS/ciRS-7, a circRNA containing about

bioRxiv preprint doi: https://doi.org/10.1101/452391; this version posted October 24, 2018. The copyright holder for this preprint (which was not certified by peer review) is the author/funder, who has granted bioRxiv a license to display the preprint in perpetuity. It is made available under aCC-BY 4.0 International license.

70 evolutionarily conserved binding sites for miRNA-7 [25,30]. Recently, CDR1AS was also found to regulate the turnover-rate of miR-7 in Cdr1as knock-out mice [31]. Certain circRNAs can regulate the expression of their linear counterparts, reducing the amount of pre-mRNA available for canonical splicing. Moreover, exon-intron circRNAs have also been described, that can interact with U1 snRNP and promote transcription of their parental genes [32]. Additionally, circRNAs binding and functionally interacting with RNA-binding proteins have been identified. For instance, circMBL, derived from the MBL/MBNL1 gene, in both D. melanogaster and humans, contains MBNL1 binding sites; MBL overexpression induces circMBL generation and this effect is dependent on the MBL binding sites [33]. Finally, a small fraction of circRNAs contains the necessary information to be translated with a cap-independent translation mechanism [26,34].

While it is well established that RNA splicing is aberrant in DM1, whether circRNA levels are dysregulated has not been explored yet. With this study, we provide the first evidence that the levels of specific circRNAs linked to myogenesis are deregulated in skeletal muscle biopsies and in myogenic cell cultures derived from DM1 patients. Due to their resistance to exonucleolytic degradation, circRNAs are generally more stable than linear RNAs, constituting an attractive new class of potential biomarkers [35]. Accordingly, here we also show that circRNAs are detectable in both peripheral blood mononuclear cells (PBMCs) and plasma derived from the blood of DM1 patients.

Methods

RNAseq and Bioinformatics Analysis

Taking advantage of the GEO repository, we analysed RNAseq data-sets derived from *tibialis anterior* muscle biopsies, taken from DM1 and control patients (GSE86356) [36]. In order to ensure sufficient sequencing depth for the identification of the expectedly rare back-splicing events, we

bioRxiv preprint doi: https://doi.org/10.1101/452391; this version posted October 24, 2018. The copyright holder for this preprint (which was not certified by peer review) is the author/funder, who has granted bioRxiv a license to display the preprint in perpetuity. It is made available under aCC-BY 4.0 International license.

used only data-sets containing more than 75 million reads (Table S1). In this way, raw reads in fastq format from 5 control and 25 DM1 ribo-depleted libraries were aligned to hg19 reference genome with BWA software (v. 0.7.12), choosing the options according to CIRI2 manual [37,38].

Subsequently, circRNAs were identified by detecting back-splice events in each of the aligned samples using CIRI2 (v. 2.0.6) with the suggested parameters. All identified circRNAs were then collected, normalized to each library size and quantified using custom R scripts. An abundance filter was applied by removing back-splice events present in <70% of either control or DM1 samples (Table S2). The circular-to-linear ratio was calculated using the highest expressed linear junction involved in the relevant back-splice event (Table S3). Briefly, we compared all annotated linear junctions that comprised either the acceptor or the donor site of the back-splice junction and kept the one with the highest amount of spliced reads. This ensured that the ratio was determined by using two equal biological entities, i.e. reads spanning a splice junction.

Patient characteristics and tissue collection

The clinical diagnosis of DM patients was based upon the criteria set by International Consortium for Myotonic Dystrophies guidelines [39]. Genetic analysis was carried out to confirm DM1 diagnosis as described previously [40]. The Muscular Impairment Rating Scale (MIRS) was used to determine the disease stage [41]. MRC scale (Medical Research Council) was used to evaluate muscle strength.

Biceps brachii muscle biopsies collected from 20 DM1 patients and 19 sex-and age matched subjects without signs of neuromuscular disorders (controls) were used for validation (Table 1).

PBMCs were isolated from the peripheral blood of 19 DM1 and 18 sex- and age matched controls (Table S4) by Ficoll-Paque™ PLUS (Ge Healthcare) gradient centrifugation as described before [42]. The plasma of 29 DM1 and 28 age-and sex- matched controls (Table S4) was collected in EDTA-tubes and cells as well as platelets were removed as described previously [43,44].

bioRxiv preprint doi: https://doi.org/10.1101/452391; this version posted October 24, 2018. The copyright holder for this preprint (which was not certified by peer review) is the author/funder, who has granted bioRxiv a license to display the preprint in perpetuity. It is made available under aCC-BY 4.0 International license.

Clinical Characteristics	DM1 (n=20)	CTRL (n=19)
Age at sampling (average ± se)	40.9 ± 3.3	38.6 ± 1.1
Sex (male/female)	10/10	15/4
MRC megascore (average ± se)	121.6 ± 1.6	130 ± 0.0
Myotonia (% of patients)	70	0
Glucose (normal values: 70–110 mg/dl)	89.9 ± 5.5	89.0 ± 3.8
Cholesterol (normal values: < 200 mg/dl)	213.8 ± 13.2	N. A.
CK	Male: 247.7 ± 42.7	N. A.
(normal values: male < 190 mg/dl. female < 125 mg/dl)	Female: 213.1 ± 63.2	N. A.
Arrhythmia (% of patients)	15.4	0
Cataract (% of patients)	7.7	0
ECG-QRS duration (normal values: 60–110 ms)	99.4 ± 3.7	N. A.
Number of CTG repeats (range)	490.6 ± 64.1 (90-1100)	N. A.
Stage of disease (range 1–5) **(% of patients at each stage)**	Stage 1: 0	N.R.
	Stage 2: 35.3	
	Stage 3: 17.6	
	Stage 4: 41.2	
	Stage 5: 5.9	

Table 1. Clinical data on DM1 and control patients used for validation in biopsies. N.R.: not relevant. N.A.: not available.

Ethical approval and informed consent

The experimental protocol was reviewed and approved by the Institutional Ethics Committee of the San Raffaele Hospital (protocol miRNADM of 23.06.2015) and was conducted according to the

bioRxiv preprint doi: https://doi.org/10.1101/452391; this version posted October 24, 2018. The copyright holder for this preprint (which was not certified by peer review) is the author/funder, who has granted bioRxiv a license to display the preprint in perpetuity. It is made available under aCC-BY 4.0 International license.

138 principles expressed in the Declaration of Helsinki, the institutional regulation and the Italian laws
139 and guidelines. A written informed consent was obtained from each patient prior to muscle biopsies
140 or blood collection.

141 Histopathological analysis

142 Muscle tissue was fresh-frozen in isopentane cooled in liquid nitrogen. Histopathological analyses
143 were performed on serial sections (8 µm) processed for routine histological or histochemical
144 stainings. Myofibrillar ATPase staining was performed as previously described, after sample pre-
145 incubation at pH 4.3, 4.6, and 10.4 [45].

146 DM1 myogenic cell lines

147 Immortalized human myotonic dystrophy muscle cell lines expressing murine *Myod1* cDNA
148 under the control of a Tet-on inducible construct were previously described [46]. Cells were
149 cultivated in DMEM growth medium (15% FBS) until confluency was reached. Myogenic
150 differentiation was induced by switching cell cultures to DMEM supplemented with 5 µg/ml insulin
151 and 4 µg/ml doxycycline (Sigma-Aldrich).

152 For silencing experiments, cells were transfected after 3 days of differentiation with 50nM
153 MBNL1/CELF1 TARGETplus SMARTpool siRNAs (Dharmacon) or with 50nM ON-
154 TARGETplus Non-targeting Pool as negative control. Cells were transfected using HiPerFect
155 reagent (Qiagen), according to manufacturer's instructions. Three days after transfection, total RNA
156 was isolated and analyzed by qPCR.

157 Isolation of total RNA

158 Total RNA was extracted from the muscle tissues using TRIzol reagent (Thermo Fisher Scientific
159 Inc.) as described previously [47,48]. For isolation of total RNA from PBMCs and cells, TRIzol
160 reagent was used according to the manufacturer's instructions. The purity and integrity of the
161 obtained RNAs were measured by Nanodrop (Thermo Fisher Scientific Inc.).

bioRxiv preprint doi: https://doi.org/10.1101/452391; this version posted October 24, 2018. The copyright holder for this preprint (which was not certified by peer review) is the author/funder, who has granted bioRxiv a license to display the preprint in perpetuity. It is made available under aCC-BY 4.0 International license.

Total RNA from plasma samples was extracted as previously described using NucleoSpin miRNA Plasma columns (Macherey-Nagel) [43,44].

Real-time reverse transcriptase qPCR

For validation experiments, total RNA was first retro-transcribed using the SuperScript Reverse Transcriptase kit (version III or IV) and then investigated by SYBR green qPCR, according to the manufacturer's protocol (Thermo Fisher Scientific Inc.). Primer couples were designed by Primer-BLAST tool (Table S5).

The relative expression was calculated using the comparative Ct method $2^{-\Delta\Delta CT}$ [49], normalizing to the averaged Cts of RPL13, RPL23 and UBC for tissue RNAs and to the averaged Cts of miR-106a and miR-17-5p for plasma RNAs [43,44].

The circular-to-linear ratio was estimated by subtracting the raw Ct of the linear transcript from the raw Ct of the corresponding circular transcript.

For score-calculations, the log2 fold changes of all significantly modulated circRNAs or circular-to-linear ratios were averaged.

Statistical Analysis.

GraphPad Prism 7.01 (GraphPad Software Inc.) was used for statistical analysis and for graph generation. Following differential expression analysis, all data-sets were checked for their distribution by D'Agostino & Pearson normality test. The only exception were the cell line data, since due to the small sample size normality test was not possible. The differential expression of circRNAs in biopsies was investigated by multiple t-test, using the recommended settings of GraphPad for false discovery rate (Benjamini, Krieger and Yekutieli) and Q= 1% as significance cut-off. For differential expression analysis of circRNAs in PBMCs, plasma and cell lines, two-tailed Student's t test or Mann Whitney was used, depending on the data-distribution. A $p < 0.05$ was deemed statistically significant. Values are expressed as ±standard error.

bioRxiv preprint doi: https://doi.org/10.1101/452391; this version posted October 24, 2018. The copyright holder for this preprint (which was not certified by peer review) is the author/funder, who has granted bioRxiv a license to display the preprint in perpetuity. It is made available under aCC-BY 4.0 International license.

Results

Identification of circRNA expression in DM1 skeletal muscle by RNA-sequencing.

Published RNA sequencing (RNAseq) data of ribo-depleted libraries derived from 5 controls and 25 DM1 *tibialis anterior* biopsies [36] were investigated for circRNA expression. Among the available data-sets, we analyzed only libraries containing at least 76 million reads, thus providing sequence information at a high depth (Table S1). By applying CIRI2 [37,38], an algorithm designed for the discovery of circRNAs, a total of 21.822 unique back-splice sites were identified across all libraries. Since most of these events were present in few samples only, a stringent abundance filter was used, resulting in ≈ 1.800 back-splice junctions (Table S2). Certain circRNAs display expression levels comparable to or even higher than their linear counterparts, suggesting a potential biological relevance [27]. To identify these particularly interesting circRNAs, the circular-to-linear ratios were estimated. Therefore, all annotated linear junctions involved with either the donor or the acceptor site of the back-splice event were quantified. The linear junction with the highest expression was then compared to the back-splice junction, revealing 578 circRNAs with a circular-to-linear ratio >0.5 in DM1 (Table S3).

To narrow the list of candidates for validation, the ≈ 1.800 identified circRNAs were intersected with a list of 29 circRNAs that were previously validated in human and mouse myoblasts [26], resulting in 18 common circRNAs (Table S3). Interestingly, most of them displayed a circular-to-linear ratio >0.5.

Validation by qPCR of differentially expressed circRNAs in DM1 skeletal muscles.

bioRxiv preprint doi: https://doi.org/10.1101/452391; this version posted October 24, 2018. The copyright holder for this preprint (which was not certified by peer review) is the author/funder, who has granted bioRxiv a license to display the preprint in perpetuity. It is made available under aCC-BY 4.0 International license.

209 Muscle tissue biopsies were harvested from *biceps brachii* of 20 DM1 and 19 sex- and age-
210 matched control individuals, with no sign of neuromuscular disorders. The DM1 group showed the
211 main characteristics of the disease, such as myotonia, cataract and muscle weakness (Table 1), as
212 well the typical histological alterations, such as central *nuclei*, high variation in fiber size, atrophic
213 fibers and nuclear clumps (Fig. S1) [1,39]. Most DM1 patients were at stage 2-4 and the
214 pathological expansions of the CTG triplets ranged from 90 to 1100.

215 Total RNAs were isolated and the expression of a set of circRNAs and their linear counterparts
216 was measured by qPCR. Out of the 18 circRNA candidates, 8 primer couples passed all technical
217 checks of specificity and efficiency. Of note, two circRNAs originated from the same gene and
218 were indicated as circRTN4 and circRTN4_03. The primers designed for circRNAs produced an
219 amplicon spanning the back-splice junction, while the linear primers resulted in amplicons crossing
220 the linear junction to a neighboring exon. Due to the key role of MBNL in DM1, the previously
221 identified circRNA hosted in the second exon of MBNL [33] and its linear form were also
222 measured. Thus, a set of 9 circRNAs together with their linear counterparts were used for validation
223 (Table S4). All tested transcripts were confirmed to be readily expressed also in *biceps brachii*
224 biopsies, with the only exception of circMBNL1 (circMBNL1), showing an expression close to the
225 detection threshold. Five circRNAs, circASPH, circCDYL, circHIPK3, circRTN4_03 and
226 circZNF609, displayed a statistically significant increase following multiple comparison testing
227 ($q<0.01$) (Fig. S2).

228 To assess whether the observed induction of the circular transcripts was simply the consequence
229 of a general increase of transcription in the relevant genomic region in DM1 patients, modulation of
230 the ratios between the circular and the linear isoforms was calculated. We identified 4 circRNAs
231 (circCDYL, circHIPK3, circRTN4_03 and circZNF609) with a significantly increased, circular-to-
232 linear ratio in DM1 muscles (Fig. 1a), implying a de-regulation of the circular transcript
233 independent from its linear counterpart. Accordingly, a similar trend was also observed in the

bioRxiv preprint doi: https://doi.org/10.1101/452391; this version posted October 24, 2018. The copyright holder for this preprint (which was not certified by peer review) is the author/funder, who has granted bioRxiv a license to display the preprint in perpetuity. It is made available under aCC-BY 4.0 International license.

RNAseq data, where the circular-to-linear ratios were higher in the DM1 affected muscles compared to the controls (Table S3).

Figure 1. Differentially modulated circular-to-linear ratios in DM1 skeletal muscles. (a) Scatterplots in log2 scale of significantly different circular-to-linear ratios identified by qPCR in DM1 muscle tissue compared to control (CTRL). After normality test, statistical significance was calculated either by t-test or Mann-Whitney test (threshold $p<0.05$), followed by correction multiple comparison, with significance threshold set at $q<0.01$. **(b)** Scatterplot of circular-to-linear ratio, estimated by averaging the log2 fold changes of significantly different circular-to-linear ratios in DM1 muscle tissue compared to control. For both panels, lines indicate mean and standard error values for each group. DM1= 20 (red dots); CTRL= 19 (black dots); **q<0.001; ***p<0.001.

DM1-circRNAs distinguish DM1 patients from controls.

To understand if the identified DM1-deregulated circRNAs (DM1-circRNAs) display a discriminating power to identify DM1 patients, Receiver Operating Characteristic (ROC) curve analysis was performed. Both, significantly increased circRNAs alone (Fig. S3) and circular-to-linear ratios (Fig. 2) were analyzed. Interestingly, with one exception (circCDYL), the discrimination power between diseased and healthy individuals increased using the circular-to-linear ratios. In detail, among the five tested ratios, ZNF609 showed the largest area under the curve (AUC= 0.92), while the others ranged between 0.84 and 0.86 (Fig. 2a). Intriguingly, averaging all five DM1-circRNA fractions into a “circular-to-linear score” (Fig. 2b) improved the performance (AUC= 0.89) with respect to the singular fractions, with the exception of circZNF609, continuing to show the largest AUC (Fig. 2a).

bioRxiv preprint doi: https://doi.org/10.1101/452391; this version posted October 24, 2018. The copyright holder for this preprint (which was not certified by peer review) is the author/funder, who has granted bioRxiv a license to display the preprint in perpetuity. It is made available under aCC-BY 4.0 International license.

In conclusion, each of the five circular-to-linear ratios, as well as the combined "circular-to-linear score" of the DM1-circRNAs are useful to discriminate healthy form diseased patients.

Figure 2. Discrimination of DM1 patients from controls using circular-to-linear ratios of DM1-circRNAs. (a) ROC curves show the sensitivity and specificity of each circRNA fraction (circ/lin) and of the combined "circular-to-linear score" to distinguish DM1 from healthy muscle tissue. **(b)** The "circular-to-linear score" was calculated by averaging the significantly modulated circular-to-linear ratios (circ/lin score, black rectangle). DM1= 20, CTRL= 19.

Correlation between DM1-circRNAs and clinical characteristics.

To evaluate a potential relationship between the deregulation of circRNAs and clinical conditions, correlation analyses were performed. One of the most clinically relevant parameters for DM1 patients is muscle strength, measured by the Medical Research Council (MRC) grading system. We found that the changes of the circular fractions of circCDYL, circHIPK3, circRTN4_03 and circZNF609 displayed a significant negative correlation to MRC (Fig. 3a). Accordingly, a negative correlation was observed also between the MRC grading and the circular-to-linear score (Fig. 3b). The strongest and most significant correlation was found for the circular fraction of ZNF609, with Pearson r= 0.57 and p=0.0002.

Collectively, these data suggest a potential of circRNAs as DM1 biomarkers, in spite of the low number of subjects analyzed.

Figure 3. Correlation of muscle strength with circular-to-linear ratios of DM1-circRNAs. (a) Pearson's correlation between significantly modulated circular-to-linear ratios identified in skeletal muscle biopsies and muscle strength measured by MRC megascore. **(b)** Pearson's correlation of the

bioRxiv preprint doi: https://doi.org/10.1101/452391; this version posted October 24, 2018. The copyright holder for this preprint (which was not certified by peer review) is the author/funder, who has granted bioRxiv a license to display the preprint in perpetuity. It is made available under aCC-BY 4.0 International license.

281 "circular-to-linear score" (obtained averaging all DM1-circRNA fractions) and muscle strength
282 measured by MRC megascore. DM1= 20 (red dots), CTRL= 19 (black dots).

283

284 DM1-circRNA levels in PBMCs and plasma of DM1 patients.

285 Since peripheral blood can be obtained with a minimally invasive procedure, it represents a
286 potentially interesting tissue for biomarker identification. Thus, we measured DM1-circRNA
287 expression in PBMCs and plasma of DM1 patients and sex- and age-matched controls. Diseased
288 and healthy subjects were chosen with the same criteria adopted for the harvesting of skeletal
289 muscle biopsies (Table S4).

290 All DM1-circRNAs were readily detectable in PBMCs, but none of them showed a significant
291 modulation (Fig. S4).

292 Among the DM1-circRNAs tested in plasma samples, circCDYL and circRTN4 were readily
293 detectable. A small, but not significant induction could be observed in DM1 patients for circCDYL
294 and circRTN4, consistent with the data obtained in biopsies (Fig. S5).

295 We conclude that the DM1-circRNA dysregulations observed in skeletal muscles are tissue
296 restricted.

297 DM1-circRNA expression in DM1 myogenic cell lines

298 We assessed whether circRNA alterations identified in DM1 muscle biopsies were also observed
299 in cultured myoblasts. To this aim, we took advantage of DM1 and control muscle cell lines
300 obtained by conversion of immortalized skin fibroblasts into multinucleated myotubes by forced
301 expression of *MyoD1* [46]. In DM1 and control differentiated myogenic cells, all circRNAs tested
302 were readily detectable. Interestingly, two of the circular transcripts, circRTN4 and circRTN4_03
303 were significantly increased in DM1 compared to control (Fig. S6). The analysis of their circular-to-
304 linear ratio confirmed the induction of circRTN4_03. Additionally, an increased circular-to-linear

bioRxiv preprint doi: https://doi.org/10.1101/452391; this version posted October 24, 2018. The copyright holder for this preprint (which was not certified by peer review) is the author/funder, who has granted bioRxiv a license to display the preprint in perpetuity. It is made available under aCC-BY 4.0 International license.

ratio was also observed for ZNF609. These results are in line with the findings obtained in DM1 biopsies (Figure 4).

We took advantage of this cell culture system to investigate whether silencing of DM1-related splicing factor affected the levels of the DM1-circRNAs modulated *in vitro*.

Since MBNL1 is impaired in DM1 patients [7,9,10], we assayed whether MBNL1 silencing in control myogenic cells induced, at least in part, the circRNA deregulations observed in DM1 myogenic cells. Control differentiated myogenic cells were transfected with MBNL1 siRNAs or relevant control oligonucleotides and RNA was extracted 3 days later. MBNL1 mRNA was significantly down modulated (Fig. S7a) and the expected alterations in the alternative-splicing patterns of SERCA1 and IR (Insulin Receptor) were observed (Fig. S7b and c) [50,51]. However, no increase was observed in the abundance of circZNF609, circRTN4 and circRTN4_03 levels (Fig. S7d).

We also tested whether the silencing of CELF1, which is activated in patients and in DM1 disease models [52], rescued DM1-circRNA expression in DM1 differentiated myogenic cells. In spite of effective CELF1 knock-down (Fig. S8a), no significant change of circZNF609, circRTN and circRTN_03 levels was observed (Fig. S8b).

We conclude that the DM1 myogenic cell lines studied reflect, at least in part, the outcome of the DM1 biopsies and therefore represent a valuable tool for functional studies *in vitro*.

Figure 4. Differentially modulated circular-to-linear ratios in myogenic cell lines. Boxplots of significantly different circular-to-linear ratios identified by qPCR in differentiated DM1 myogenic cells compared to controls (*p<0.05; **p<0.01; DM1= 4; CTRL= 4).

bioRxiv preprint doi: https://doi.org/10.1101/452391; this version posted October 24, 2018. The copyright holder for this preprint (which was not certified by peer review) is the author/funder, who has granted bioRxiv a license to display the preprint in perpetuity. It is made available under aCC-BY 4.0 International license.

Discussion

A molecular hallmark of DM1 is the dysregulation of alternative splicing, affecting many genes involved in muscle homeostasis and function [16,17,53]. CircRNAs are indeed alternative splicing products [20,21] and, in this proof-of-principle study, we provide evidence of de-regulation of circRNA expression in DM1 patients. We analyzed 30 publicly available gene-expression data-sets of DM1 and control *tibialis anterior* muscles [36], using bioinformatics tools designed for the identification of circRNA-specific back-splice events. Applying stringent selection and abundance filters, we identified ≈ 1.800 unique circular splicing events, a number comparable to circRNAs found to be expressed in human myoblasts and myotubes [26].

During the testing phase of the bioinformatics pipeline with other data-sets, we performed several attempts of differential expression analysis (data not shown). Unfortunately, performances obtained were largely unsatisfactory, likely due to very low read numbers for most circRNA species and to normalization difficulties. Therefore, in this study we chose another approach for the identification of circRNAs potentially relevant in DM1. We filtered for circRNAs displaying expression across many samples and then selected circRNAs previously shown to be involved in myogenesis [26]. Of note, most of these circRNAs also displayed a high circular-to-linear ratio. This suggests that these circRNAs are not a mere by-product of the transcript maturation process, and might also indicate an independent regulation as well as an additional biological function.

For opportunity reasons, the validation step was performed in *biceps brachii* biopsies, since only for this muscle type a sufficient number of samples was available to us. It should be acknowledged that *biceps brachii* is generally less severely affected than other distal muscles in DM1 patients [1-3,39]. Thus, some of the circRNA level differences that failed to reach statistical significance in our validation analysis, might be indeed relevant in distal muscles. On the other side, it is plausible to hypothesize that circRNA alterations identified in proximal muscles could be more pronounced in distal muscles.

bioRxiv preprint doi: https://doi.org/10.1101/452391; this version posted October 24, 2018. The copyright holder for this preprint (which was not certified by peer review) is the author/funder, who has granted bioRxiv a license to display the preprint in perpetuity. It is made available under aCC-BY 4.0 International license.

In spite of the preliminary and not-comprehensive nature of this study, we found that the levels of 5 out of 9 circRNAs tested were significantly increased, suggesting a potentially pervasive dysregulation of circRNAs in DM1. Accordingly, 4 of these circRNAs also displayed an increased circular-to-linear ratio. The most likely interpretation of these alterations is that they are caused by the dysfunction of the alternative splicing machinery characterizing DM1 [16,17,53]. Silencing of either MBNL1 or CELF1 in control and DM1 cultured myotubes did not affect the abundance of circZNF609, circRTN4 and circRTN4_03. While negative data should always be evaluated in a very cautious manner, one possible interpretation is that other splicing factors, such as different MBNL-family members, Staufen1 and DDX5 [6-12], regulate the generation of the DM1-circRNAs. Moreover, these splicing factors might be redundant in circRNA regulation, making the silencing of a single splicing factor ineffective. Finally, higher stability of circRNAs compared to their linear counterparts [54] should also be considered as possible mechanism underpinning the increase of the circular-to-linear ratio of DM1-circRNAs.

CircRNA dysregulation may lead to pathological consequences to be investigated. In this respect, however, little is known of the identified DM1-circRNAs. CircHIPK3 positively regulates human cell growth by sponging multiple miRNAs [55,56]. Among these miRNAs, there are miR-29b and miR-193a. Intriguingly, both miRNAs were previously found to be down-modulated in DM1 [57] and DM2, respectively [47]. CircHIPK3 levels are also increased in retinal endothelial cells exposed to diabetes-related stressors, in retinas of diabetic mice and in the plasma of diabetic patients. Moreover, in retinal endothelial-cells, circHIPK3 affects cell viability, proliferation, migration, and function [58]. While the implication of circHIPK3 in DM1 should be investigated, it is worth noting that insulin resistance is very often present in DM1 patients [1-3,59].

CircZNF609 is downregulated during myogenesis and can specifically control myoblast proliferation [26]. Moreover, its mouse homologue circZfp609 suppresses myogenic differentiation [60]. Of note, circZNF609 is elevated in Duchenne muscular dystrophy myoblasts, indicating that

bioRxiv preprint doi: https://doi.org/10.1101/452391; this version posted October 24, 2018. The copyright holder for this preprint (which was not certified by peer review) is the author/funder, who has granted bioRxiv a license to display the preprint in perpetuity. It is made available under aCC-BY 4.0 International license.

379 the DM1-circRNAs identified in this study might be deregulated in other muscular diseases. Like
380 circHIPK3, also circZNF609 is induced by high glucose *in vivo* and *in vitro* and regulates the
381 function of retinal endothelial cells [61].

382 Finally, the host gene of circRTN4 displays muscle-specific splicing [62]. It is a direct target of
383 RBM20, an alternative-splicing regulator of cardiac genes, associated with coronary heart disease.
384 Mutation of RBM20 results in altered splicing of its target genes, causing the retention of specific
385 exons of RTN4 mRNA. Since RBM20 is also expressed and active in skeletal muscles [63], further
386 investigations are needed to assess the potential involvement of RBM20 also in circRTN4
387 formation.

388 Ashwal-Fluss and collaborators [33], by studying circRNAs identified in neuronal tissues,
389 reported that the second exon of the splicing factor *MBLN1* (*MBL* in drosophila) is circularized in
390 flies and humans and that circMBL production competes with canonical pre-mRNA splicing.
391 Moreover, Muscleblind protein interacts with flanking introns of its own gene to promote exon
392 circularization. This observation prompted us to measure circMBNL1 in skeletal muscle biopsies
393 and PBMCs of DM1 patients, where MBNL1 protein bioavailability is reduced by its sequestration
394 in nuclear CUG-foci [9,10]. However, we did not observe any modulation of circMBNL1 in these
395 tissues. The most likely explanation is that circMBNL1 regulation is highly context specific.
396 Indeed, while in fly heads, this circRNA is more abundant than the linear counterpart, the opposite
397 seems to be true in human skeletal muscle, where RNAseq data indicated a circular-to-linear ratio
398 of 0.05 (Table S3). In keeping with this hypothesis, very low circMBL levels were also observed in
399 drosophila S2 cells [33]. Furthermore, changes in the splicing pattern of MBNL1 mRNA
400 (comprising or not exon1) were observed in cardiac and skeletal muscles, but not in the brain of
401 DM1 patients compared to controls [64,65], confirming a high tissue-specificity in the regulation of
402 MBNL1 transcript.

bioRxiv preprint doi: https://doi.org/10.1101/452391; this version posted October 24, 2018. The copyright holder for this preprint (which was not certified by peer review) is the author/funder, who has granted bioRxiv a license to display the preprint in perpetuity. It is made available under aCC-BY 4.0 International license.

Identification of diagnostic and prognostic biomarkers is an unmet clinical need for DM1 patients. Recent studies suggest that alternative splicing isoforms in skeletal muscle tissue have a high potential as biomarkers of DM severity and for the monitoring of therapeutic responses [53]. Due to their loop-structure, circRNAs are highly resistant to exonucleases [54], holding a great potential as disease biomarkers. Promisingly, the potential of circRNAs as molecular markers has been highlighted recently in various types of cancer [66], measuring circRNAs not only in biopsies of solid tissues, but also in extracellular compartments, such as serum or exosomes [66,67].

It is still too early to conclude whether circRNAs will find their way to the clinic. This will largely depend on both technical issues, such as detectability and stability of circRNAs in biological samples, as well as on whether circRNAs are functional elements of the molecular mechanisms driving the disease or mere byproducts [54].While further studies are obviously needed, we found that the circular-to-linear ratios as well as the combined "circular-to-linear score" of the DM1-circRNAs in skeletal muscle biopsies accurately discriminated healthy form DM1 patients. Moreover, a correlation between the MRC grading and the circular-to-linear score could be identified. Additional investigations are needed to evaluate the potential of circRNAs as DM1 biomarker, involving a higher number of subjects. Comparison with other myopathies will also allow to investigate their possible disease-specificity.

CircRNAs are detectable also in the peripheral blood that can be harvested with minimally-invasive techniques. Indeed, DM1-circRNAs were measured both in PBMCs and, at least in part, in plasma samples. On the one side, the high context-dependent regulation of circRNAs implicates that the pattern of expression observed in the peripheral blood is unlikely to mirror that of other tissues, such as the skeletal muscle. On the other side, the apparent pervasiveness of circRNA dysregulation suggest that comprehensive screenings of circRNAs might indeed succeed in the identification of common circRNAs between blood and affected organs. An alternative approach

bioRxiv preprint doi: https://doi.org/10.1101/452391; this version posted October 24, 2018. The copyright holder for this preprint (which was not certified by peer review) is the author/funder, who has granted bioRxiv a license to display the preprint in perpetuity. It is made available under aCC-BY 4.0 International license.

427 may be represented by the analysis of urine extracellular RNAs, whose splice variants have been
428 shown to discriminate DM1 patients efficiently [68].

429 Acknowledgments

430 We thank the platform for immortalization of human cells of the Institut de Myologie, Paris, France,
431 for providing DM1 and control myogenic cell lines and Michele Cavalli (Biomedical Sciences for
432 Health, University of Milan and IRCCS Policlinico San Donato, Milan, Italy) for his support in
433 clinical data collection.

434

435 References

436 1. Meola G, Cardani R. Myotonic dystrophies: An update on clinical aspects, genetic, pathology,
437 and molecular pathomechanisms. Biochim Biophys Acta. 2015;1852: 594-606.
438 2. De Antonio M, Dogan C, Hamroun D, Mati M, Zerrouki S, Eymard B, et al. Unravelling the
439 myotonic dystrophy type 1 clinical spectrum: A systematic registry-based study with implications for
440 disease classification. Rev Neurol (Paris). 2016;172: 572-580.
441 3. Gagnon C, Chouinard MC, Laberge L, Veillette S, Begin P, Breton R, et al. Health supervision
442 and anticipatory guidance in adult myotonic dystrophy type 1. Neuromuscul Disord. 2010;20: 847-
443 851.
444 4. Gourdon G, Meola G. Myotonic Dystrophies: State of the Art of New Therapeutic Developments
445 for the CNS. Front Cell Neurosci. 2017;11: 101.
446 5. Fu YH, Pizzuti A, Fenwick RG,Jr, King J, Rajnarayan S, Dunne PW, et al. An unstable triplet
447 repeat in a gene related to myotonic muscular dystrophy. Science. 1992;255: 1256-1258.
448 6. Bondy-Chorney E, Crawford Parks TE, Ravel-Chapuis A, Klinck R, Rocheleau L, Pelchat M, et
449 al. Staufen1 Regulates Multiple Alternative Splicing Events either Positively or Negatively in DM1
450 Indicating Its Role as a Disease Modifier. PLoS Genet. 2016;12: e1005827.

bioRxiv preprint doi: https://doi.org/10.1101/452391; this version posted October 24, 2018. The copyright holder for this preprint (which was not certified by peer review) is the author/funder, who has granted bioRxiv a license to display the preprint in perpetuity. It is made available under aCC-BY 4.0 International license.

451 7. Lin X, Miller JW, Mankodi A, Kanadia RN, Yuan Y, Moxley RT, et al. Failure of MBNL1-
452 dependent post-natal splicing transitions in myotonic dystrophy. Hum Mol Genet. 2006;15: 2087-
453 2097.
454 8. Laurent FX, Sureau A, Klein AF, Trouslard F, Gasnier E, Furling D, et al. New function for the
455 RNA helicase p68/DDX5 as a modifier of MBNL1 activity on expanded CUG repeats. Nucleic Acids
456 Res. 2012;40: 3159-3171.
457 9. Dansithong W, Paul S, Comai L, Reddy S. MBNL1 is the primary determinant of focus formation
458 and aberrant insulin receptor splicing in DM1. J Biol Chem. 2005;280: 5773-5780.
459 10. Miller JW, Urbinati CR, Teng-Umnuay P, Stenberg MG, Byrne BJ, Thornton CA, et al.
460 Recruitment of human muscleblind proteins to (CUG)(n) expansions associated with myotonic
461 dystrophy. EMBO J. 2000;19: 4439-4448.
462 11. Philips AV, Timchenko LT, Cooper TA. Disruption of splicing regulated by a CUG-binding
463 protein in myotonic dystrophy. Science. 1998;280: 737-741.
464 12. Timchenko LT, Miller JW, Timchenko NA, DeVore DR, Datar KV, Lin L, et al. Identification
465 of a (CUG)n triplet repeat RNA-binding protein and its expression in myotonic dystrophy. Nucleic
466 Acids Res. 1996;24: 4407-4414.
467 13. Chen KY, Pan H, Lin MJ, Li YY, Wang LC, Wu YC, et al. Length-dependent toxicity of
468 untranslated CUG repeats on Caenorhabditis elegans. Biochem Biophys Res Commun. 2007;352:
469 774-779.
470 14. Garcia-Lopez A, Monferrer L, Garcia-Alcover I, Vicente-Crespo M, Alvarez-Abril MC, Artero
471 RD. Genetic and chemical modifiers of a CUG toxicity model in Drosophila. PLoS One. 2008;3:
472 e1595.
473 15. Mankodi A, Logigian E, Callahan L, McClain C, White R, Henderson D, et al. Myotonic
474 dystrophy in transgenic mice expressing an expanded CUG repeat. Science. 2000;289: 1769-1773.

bioRxiv preprint doi: https://doi.org/10.1101/452391; this version posted October 24, 2018. The copyright holder for this preprint (which was not certified by peer review) is the author/funder, who has granted bioRxiv a license to display the preprint in perpetuity. It is made available under aCC-BY 4.0 International license.

475 16. Du H, Cline MS, Osborne RJ, Tuttle DL, Clark TA, Donohue JP, et al. Aberrant alternative
476 splicing and extracellular matrix gene expression in mouse models of myotonic dystrophy. Nat Struct
477 Mol Biol. 2010;17: 187-193.
478 17. Kalsotra A, Xiao X, Ward AJ, Castle JC, Johnson JM, Burge CB, et al. A postnatal switch of
479 CELF and MBNL proteins reprograms alternative splicing in the developing heart. Proc Natl Acad
480 Sci U S A. 2008;105: 20333-20338.
481 18. Kanadia RN, Johnstone KA, Mankodi A, Lungu C, Thornton CA, Esson D, et al. A muscleblind
482 knockout model for myotonic dystrophy. Science. 2003;302: 1978-1980.
483 19. Batra R, Charizanis K, Manchanda M, Mohan A, Li M, Finn DJ, et al. Loss of MBNL leads to
484 disruption of developmentally regulated alternative polyadenylation in RNA-mediated disease. Mol
485 Cell. 2014;56: 311-322.
486 20. Noh JH, Kim KM, McClusky WG, Abdelmohsen K, Gorospe M. Cytoplasmic functions of long
487 noncoding RNAs. Wiley Interdiscip Rev RNA. 2018;9: e1471.
488 21. Holdt LM, Kohlmaier A, Teupser D. Molecular roles and function of circular RNAs in
489 eukaryotic cells. Cell Mol Life Sci. 2018;75: 1071-1098.
490 22. Du WW, Zhang C, Yang W, Yong T, Awan FM, Yang BB. Identifying and Characterizing
491 circRNA-Protein Interaction. Theranostics. 2017;7: 4183-4191.
492 23. Carrara M, Fuschi P, Ivan C, Martelli F. Circular RNAs: Methodological challenges and
493 perspectives in cardiovascular diseases. J Cell Mol Med. 2018.
494 24. Jeck WR, Sorrentino JA, Wang K, Slevin MK, Burd CE, Liu J, et al. Circular RNAs are
495 abundant, conserved, and associated with ALU repeats. RNA. 2013;19: 141-157.
496 25. Memczak S, Jens M, Elefsinioti A, Torti F, Krueger J, Rybak A, et al. Circular RNAs are a large
497 class of animal RNAs with regulatory potency. Nature. 2013;495: 333-338.
498 26. Legnini I, Di Timoteo G, Rossi F, Morlando M, Briganti F, Sthandier O, et al. Circ-ZNF609 Is
499 a Circular RNA that Can Be Translated and Functions in Myogenesis. Mol Cell. 2017;66: 22-37.e9.

bioRxiv preprint doi: https://doi.org/10.1101/452391; this version posted October 24, 2018. The copyright holder for this preprint (which was not certified by peer review) is the author/funder, who has granted bioRxiv a license to display the preprint in perpetuity. It is made available under aCC-BY 4.0 International license.

500 27. Salzman J, Gawad C, Wang PL, Lacayo N, Brown PO. Circular RNAs are the predominant
501 transcript isoform from hundreds of human genes in diverse cell types. PLoS One. 2012;7: e30733.
502 28. Rybak-Wolf A, Stottmeister C, Glazar P, Jens M, Pino N, Giusti S, et al. Circular RNAs in the
503 Mammalian Brain Are Highly Abundant, Conserved, and Dynamically Expressed. Mol Cell.
504 2015;58: 870-885.
505 29. Wei X, Li H, Yang J, Hao D, Dong D, Huang Y, et al. Circular RNA profiling reveals an
506 abundant circLMO7 that regulates myoblasts differentiation and survival by sponging miR-378a-3p.
507 Cell Death Dis. 2017;8: e3153.
508 30. Hansen TB, Jensen TI, Clausen BH, Bramsen JB, Finsen B, Damgaard CK, et al. Natural RNA
509 circles function as efficient microRNA sponges. Nature. 2013;495: 384-388.
510 31. Piwecka M, Glazar P, Hernandez-Miranda LR, Memczak S, Wolf SA, Rybak-Wolf A, et al.
511 Loss of a mammalian circular RNA locus causes miRNA deregulation and affects brain function.
512 Science. 2017;357: 10.1126/science.aam8526. Epub 2017 Aug 10.
513 32. Li Z, Huang C, Bao C, Chen L, Lin M, Wang X, et al. Exon-intron circular RNAs regulate
514 transcription in the nucleus. Nat Struct Mol Biol. 2015;22: 256-264.
515 33. Ashwal-Fluss R, Meyer M, Pamudurti NR, Ivanov A, Bartok O, Hanan M, et al. circRNA
516 biogenesis competes with pre-mRNA splicing. Mol Cell. 2014;56: 55-66.
517 34. Pamudurti NR, Bartok O, Jens M, Ashwal-Fluss R, Stottmeister C, Ruhe L, et al. Translation of
518 CircRNAs. Mol Cell. 2017;66: 9-21.e7.
519 35. Yang Z, Xie L, Han L, Qu X, Yang Y, Zhang Y, et al. Circular RNAs: Regulators of Cancer-
520 Related Signaling Pathways and Potential Diagnostic Biomarkers for Human Cancers. Theranostics.
521 2017;7: 3106-3117.
522 36. Wagner SD, Struck AJ, Gupta R, Farnsworth DR, Mahady AE, Eichinger K, et al. Dose-
523 Dependent Regulation of Alternative Splicing by MBNL Proteins Reveals Biomarkers for Myotonic
524 Dystrophy. PLoS Genet. 2016;12: e1006316.

bioRxiv preprint doi: https://doi.org/10.1101/452391; this version posted October 24, 2018. The copyright holder for this preprint (which was not certified by peer review) is the author/funder, who has granted bioRxiv a license to display the preprint in perpetuity. It is made available under aCC-BY 4.0 International license.

525 37. Gao Y, Wang J, Zhao F. CIRI: an efficient and unbiased algorithm for de novo circular RNA
526 identification. Genome Biol. 2015;16: 4-014-0571-3.
527 38. Gao Y, Zhang J, Zhao F. Circular RNA identification based on multiple seed matching. Brief
528 Bioinform. 2017.
529 39. Udd B, Meola G, Krahe R, Thornton C, Ranum LP, Bassez G, et al. 140th ENMC International
530 Workshop: Myotonic Dystrophy DM2/PROMM and other myotonic dystrophies with guidelines on
531 management. Neuromuscul Disord. 2006;16: 403-413.
532 40. Valaperta R, Sansone V, Lombardi F, Verdelli C, Colombo A, Valisi M, et al. Identification and
533 characterization of DM1 patients by a new diagnostic certified assay: neuromuscular and cardiac
534 assessments. Biomed Res Int. 2013;2013: 958510.
535 41. Mathieu J, Boivin H, Meunier D, Gaudreault M, Begin P. Assessment of a disease-specific
536 muscular impairment rating scale in myotonic dystrophy. Neurology. 2001;56: 336-340.
537 42. Voellenkle C, van Rooij J, Cappuzzello C, Greco S, Arcelli D, Di Vito L, et al. MicroRNA
538 signatures in peripheral blood mononuclear cells of chronic heart failure patients. Physiol Genomics.
539 2010;42: 420-426.
540 43. Perfetti A, Greco S, Bugiardini E, Cardani R, Gaia P, Gaetano C, et al. Plasma microRNAs as
541 biomarkers for myotonic dystrophy type 1. Neuromuscul Disord. 2014;24: 509-515.
542 44. Perfetti A, Greco S, Cardani R, Fossati B, Cuomo G, Valaperta R, et al. Validation of plasma
543 microRNAs as biomarkers for myotonic dystrophy type 1. Sci Rep. 2016;6: 38174.
544 45. Dubowitz V. Muscle biopsy: A Practical Approach. In: Anonymous Muscle biopsy: A Practical
545 Approach. London: Bailliere Tindall: Dubowitz, Victor; 1985. pp. 19-40.
546 46. Arandel L, Polay Espinoza M, Matloka M, Bazinet A, De Dea Diniz D, Naouar N, et al.
547 Immortalized human myotonic dystrophy muscle cell lines to assess therapeutic compounds. Dis
548 Model Mech. 2017;10: 487-497.
549 47. Greco S, Perfetti A, Fasanaro P, Cardani R, Capogrossi MC, Meola G, et al. Deregulated
550 microRNAs in myotonic dystrophy type 2. PLoS One. 2012;7: e39732.

bioRxiv preprint doi: https://doi.org/10.1101/452391; this version posted October 24, 2018. The copyright holder for this preprint (which was not certified by peer review) is the author/funder, who has granted bioRxiv a license to display the preprint in perpetuity. It is made available under aCC-BY 4.0 International license.

551 48. Greco S, De Simone M, Colussi C, Zaccagnini G, Fasanaro P, Pescatori M, et al. Common
552 micro-RNA signature in skeletal muscle damage and regeneration induced by Duchenne muscular
553 dystrophy and acute ischemia. FASEB J. 2009;23: 3335-3346.
554 49. Livak KJ, Schmittgen TD. Analysis of relative gene expression data using real-time quantitative
555 PCR and the 2(-Delta Delta C(T)) Method. Methods. 2001;25: 402-408.
556 50. Kimura T, Nakamori M, Lueck JD, Pouliquin P, Aoike F, Fujimura H, et al. Altered mRNA
557 splicing of the skeletal muscle ryanodine receptor and sarcoplasmic/endoplasmic reticulum Ca2+-
558 ATPase in myotonic dystrophy type 1. Hum Mol Genet. 2005;14: 2189-2200.
559 51. Savkur RS, Philips AV, Cooper TA. Aberrant regulation of insulin receptor alternative splicing
560 is associated with insulin resistance in myotonic dystrophy. Nat Genet. 2001;29: 40-47.
561 52. Wang ET, Ward AJ, Cherone JM, Giudice J, Wang TT, Treacy DJ, et al. Antagonistic regulation
562 of mRNA expression and splicing by CELF and MBNL proteins. Genome Res. 2015;25: 858-871.
563 53. Nakamori M, Sobczak K, Puwanant A, Welle S, Eichinger K, Pandya S, et al. Splicing
564 biomarkers of disease severity in myotonic dystrophy. Ann Neurol. 2013;74: 862-872.
565 54. Ebbesen KK, Kjems J, Hansen TB. Circular RNAs: Identification, biogenesis and function.
566 Biochim Biophys Acta. 2016;1859: 163-168.
567 55. Zheng Q, Bao C, Guo W, Li S, Chen J, Chen B, et al. Circular RNA profiling reveals an abundant
568 circHIPK3 that regulates cell growth by sponging multiple miRNAs. Nat Commun. 2016;7: 11215.
569 56. Liu X, Liu B, Zhou M, Fan F, Yu M, Gao C, et al. Circular RNA HIPK3 regulates human lens
570 epithelial cells proliferation and apoptosis by targeting the miR-193a/CRYAA axis. Biochem
571 Biophys Res Commun. 2018;503: 2277-2285.
572 57. Perbellini R, Greco S, Sarra-Ferraris G, Cardani R, Capogrossi MC, Meola G, et al.
573 Dysregulation and cellular mislocalization of specific miRNAs in myotonic dystrophy type 1.
574 Neuromuscul Disord. 2011;21: 81-88.
575 58. Shan K, Liu C, Liu BH, Chen X, Dong R, Liu X, et al. Circular Noncoding RNA HIPK3
576 Mediates Retinal Vascular Dysfunction in Diabetes Mellitus. Circulation. 2017;136: 1629-1642.

bioRxiv preprint doi: https://doi.org/10.1101/452391; this version posted October 24, 2018. The copyright holder for this preprint (which was not certified by peer review) is the author/funder, who has granted bioRxiv a license to display the preprint in perpetuity. It is made available under aCC-BY 4.0 International license.

577 59. Renna LV, Bose F, Iachettini S, Fossati B, Saraceno L, Milani V, et al. Receptor and post-
578 receptor abnormalities contribute to insulin resistance in myotonic dystrophy type 1 and type 2
579 skeletal muscle. PLoS One. 2017;12: e0184987.
580 60. Wang Y, Li M, Wang Y, Liu J, Zhang M, Fang X, et al. A Zfp609 circular RNA regulates
581 myoblast differentiation by sponging miR-194-5p. Int J Biol Macromol. 2018.
582 61. Liu C, Yao MD, Li CP, Shan K, Yang H, Wang JJ, et al. Silencing Of Circular RNA-ZNF609
583 Ameliorates Vascular Endothelial Dysfunction. Theranostics. 2017;7: 2863-2877.
584 62. Maatz H, Jens M, Liss M, Schafer S, Heinig M, Kirchner M, et al. RNA-binding protein RBM20
585 represses splicing to orchestrate cardiac pre-mRNA processing. J Clin Invest. 2014;124: 3419-3430.
586 63. Chen Z, Maimaiti R, Zhu C, Cai H, Stern A, Mozdziak P, et al. Z-band and M-band titin splicing
587 and regulation by RNA binding motif 20 in striated muscles. J Cell Biochem. 2018.
588 64. Konieczny P, Stepniak-Konieczna E, Sobczak K. MBNL proteins and their target RNAs,
589 interaction and splicing regulation. Nucleic Acids Res. 2014;42: 10873-10887.
590 65. Konieczny P, Stepniak-Konieczna E, Taylor K, Sznajder LJ, Sobczak K. Autoregulation of
591 MBNL1 function by exon 1 exclusion from MBNL1 transcript. Nucleic Acids Res. 2017;45: 1760-
592 1775.
593 66. Kristensen LS, Hansen TB, Veno MT, Kjems J. Circular RNAs in cancer: opportunities and
594 challenges in the field. Oncogene. 2018;37: 555-565.
595 67. Li Y, Zheng Q, Bao C, Li S, Guo W, Zhao J, et al. Circular RNA is enriched and stable in
596 exosomes: a promising biomarker for cancer diagnosis. Cell Res. 2015;25: 981-984.
597 68. Antoury L, Hu N, Balaj L, Das S, Georghiou S, Darras B, et al. Analysis of extracellular mRNA
598 in human urine reveals splice variant biomarkers of muscular dystrophies. Nat Commun. 2018;9:
599 3906-018-06206-0.
600
601

bioRxiv preprint doi: https://doi.org/10.1101/452391; this version posted October 24, 2018. The copyright holder for this preprint (which was not certified by peer review) is the author/funder, who has granted bioRxiv a license to display the preprint in perpetuity. It is made available under aCC-BY 4.0 International license.

Supporting information

Figure S1. Histopathological analysis of *biceps brachii* biopsies obtained from a representative DM1 patient (a, b) and from a representative control (c). In DM1 patient, Hematoxylin & Eosin **(a)** and ATPase pH 10.4 **(b)** stainings displayed the characteristic histopathological features of DM1, such as central nuclei (asterisks), atrophic fibers (arrow) and an evident fiber size variability both of type 1 (negative fibers) and type 2 (brown fibers) fibers.

Figure S2. Significantly modulated circRNAs in DM1 skeletal muscles. Scatterplots of circRNA (circ.) transcripts identified by qPCR as differentially expressed in DM1 *biceps brachii* biopsies are shown together with their linear counterparts (lin.). Lines indicate mean and standard error values for each group. After normality test, statistical significance was calculated either by t-test or Mann-Whitney test (threshold $p<0.05$), followed by correction multiple comparison, with significance threshold set at $q<0.01$ (*$q<0.01$; **$q<0.001$). DM1= 20 (red dots), Controls= 19 (CTRL, black dots).

Figure S3. Discrimination of DM1 from healthy patients by circRNA modulation. ROC curves show the sensitivity and specificity of each DM1-circRNA to distinguish DM1 from healthy muscle tissue. DM1= 20, CTRL= 19.

Figure S4. DM1-circRNA levels in PBMCs derived from DM1 patients and controls. RNA was extracted from PBMCs of DM1 and control individuals. Scatterplots show the levels of DM1-circRNAs detected by qPCR. DM1= 19 (red dots), Controls= 18 (CTRL, black dots). Lines indicate mean and standard error values for each group.

Figure S5. DM1-circRNA levels in plasma derived from DM1 patients and controls. RNA was extracted from platelet-free plasma of DM1 and control individuals. Scatterplots show the levels of circRNAs detectable by qPCR. DM1= 29 (red dots), Controls= 28 (CTRL, black dots). Lines indicate mean and standard error values for each group.

bioRxiv preprint doi: https://doi.org/10.1101/452391; this version posted October 24, 2018. The copyright holder for this preprint (which was not certified by peer review) is the author/funder, who has granted bioRxiv a license to display the preprint in perpetuity. It is made available under aCC-BY 4.0 International license.

Figure S6. Significantly modulated circRNAs in DM1 myogenic cell lines. Boxplots of differentially expressed circRNAs (circ.) and their linear counterparts (lin.) identified by qPCR in differentiated DM1 myogenic cells compared to controls (*p<0.05; **p<0.01; DM1= 4; CTRL= 4).

Figure S7. MBNL1 silencing does not affect DM1-circRNA levels. Differentiated control myogenic cells were transfected with siRNAs targeting MBNL1 or with control siRNAs (n=5). (**a**) Efficiency of MBNL1 knock-down was assessed by qPCR (*** p<0.0001). (**b** and **c**) MBNL1 silencing induced the expected increases of the SERCA1 isoform excluding exon 22 (isoform b), and of the IR isoform excluding exon 11 (isoform a), as assessed by PCR followed by agarose gel electrophoresis. Representative gels are shown. (**d**) circZNF609, circRTN4 and circRTN4_03 levels were measured by qPCR. None of the circRNAs displayed a statistically significant increase.

Figure S8. CELF1 silencing does not affect DM1-circRNA levels. Differentiated DM1 myogenic cells were transfected with siRNAs targeting CELF1 or with control siRNAs (n=3). (**a**) Efficiency of CELF1 knock-down was assessed by qPCR (*** p<0.0001). (**b**) circZNF609, circRTN4 and circRTN4_03 levels were measured by qPCR. None of the circRNAs displayed a statistically significant decrease.

Table S1. Library size of publicly available data-sets used for circRNA identification in DM1 skeletal muscle by RNAseq. A set of 30 transcriptomes (25 DM1 and 5 healthy controls) from human tibialis biopsies (GSE86356) was investigated for back-splice events. The sequencing depth is reported as million sequenced reads after mapping to the human genome version hg19. Each data-set is identified by its SRA Run number; controls are highlighted in grey.

Table S2. circRNA identification and expression in DM1 skeletal muscle by RNAseq. Normalized counts of 1797 different circRNA species identified by CIRI2-algorithm, following a filtering step for abundance. Each back-splice junction is identified with the coordinates of the

bioRxiv preprint doi: https://doi.org/10.1101/452391; this version posted October 24, 2018. The copyright holder for this preprint (which was not certified by peer review) is the author/funder, who has granted bioRxiv a license to display the preprint in perpetuity. It is made available under aCC-BY 4.0 International license.

649 involved donor and acceptor sites in the format "chromosome number: donor position | acceptor
650 position". Each data-set is identified by its SRA Run number, controls are highlighted in grey.

651 **Table S3. Ratios of circular versus linear expression levels measured in DM1 skeletal muscle**
652 **by RNAseq.** For estimation of circular-to-linear ratios, the linear junction with the highest coverage
653 involved with either the donor or the acceptor site of the back-splice event was determined. The
654 averaged, normalized counts across all libraries in each condition were calculated for linear and back-
655 splice junction. The circular-to-linear ratios were determined for controls and DM1 and are here
656 highlighted in grey. Additionally, the circRNAs identified in human tibialis biopsies were intersected
657 with myogenic circRNAs identified by Legnini et al. [26] The final validation set chosen for qPCR
658 is displayed in the column "Validation-set".

659 **Table S4. Clinical data of DM1 patients and controls used for circRNA detection in plasma**
660 **and PBMCs.** NR: not relevant, NA: not available.

661 **Table S5. Primer-sequences.** List of primer-couples used for relative quantification of circRNAs
662 and their linear counterparts by qPCR. With the exception of CDYL and HIPK3, circular transcripts
663 and their linear counterparts shared one primer, either forward or reverse.

a

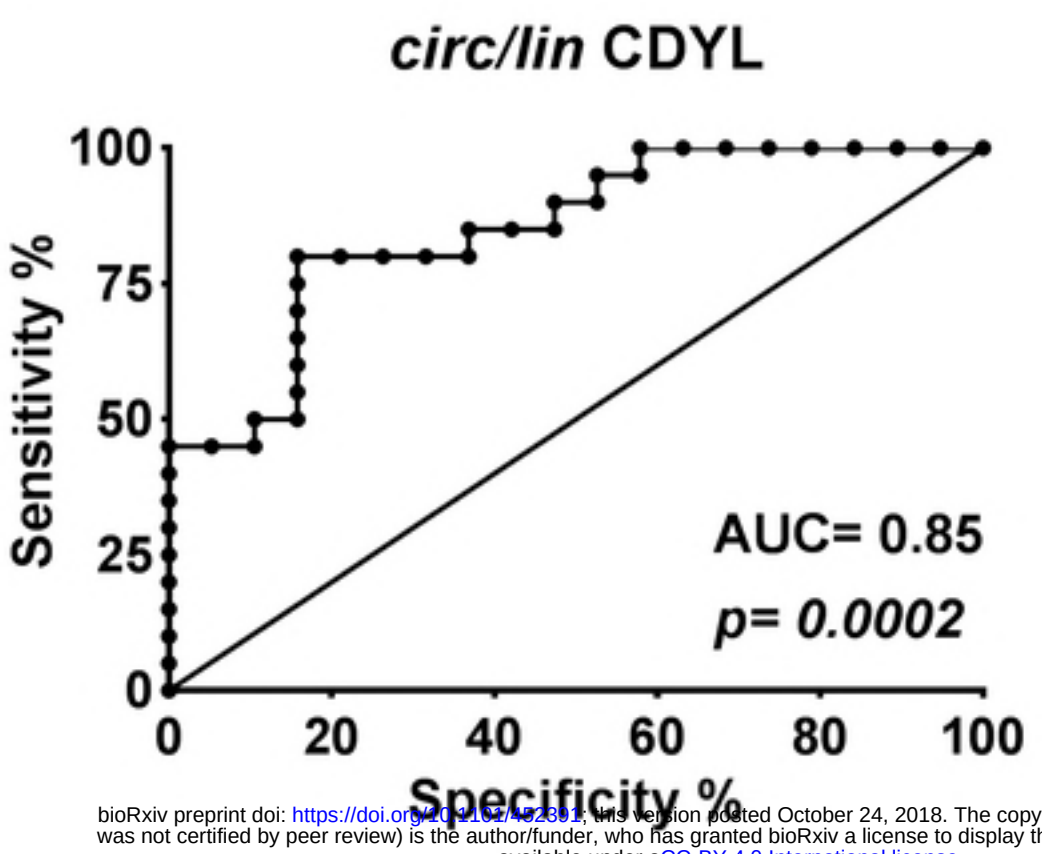

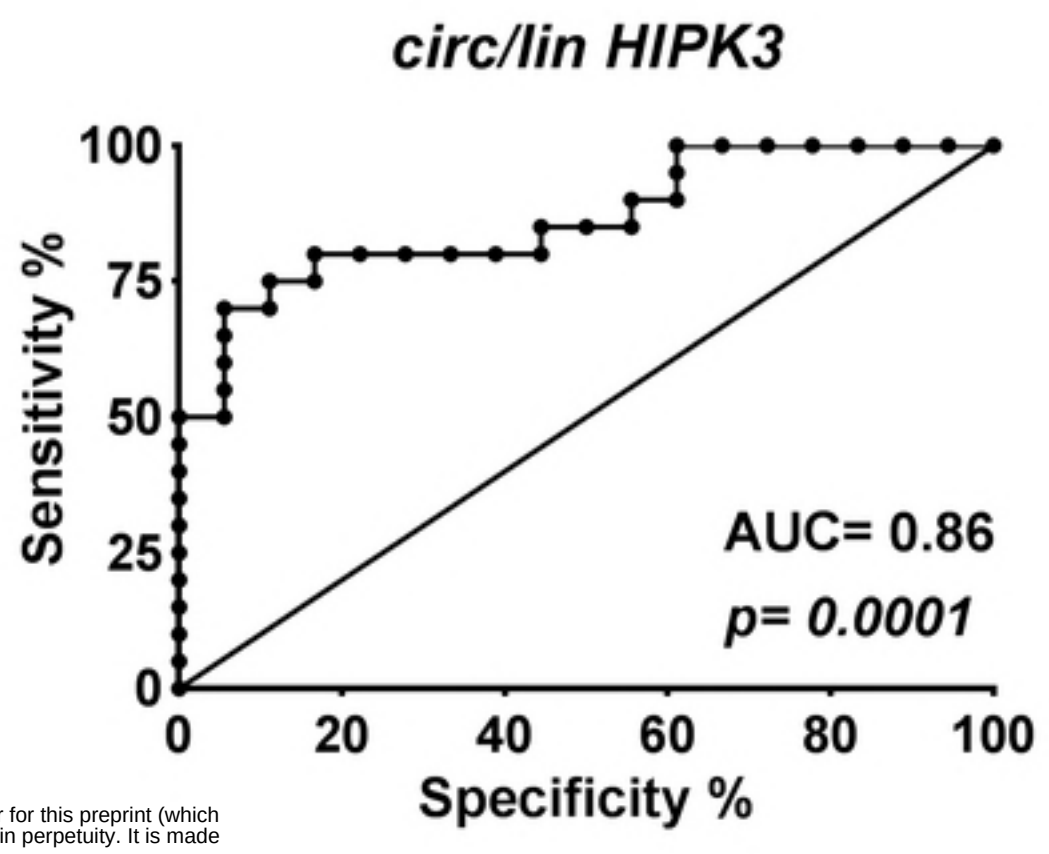

bioRxiv preprint doi: https://doi.org/10.1101/452301; this version posted October 24, 2018. The copyright holder for this preprint (which was not certified by peer review) is the author/funder, who has granted bioRxiv a license to display the preprint in perpetuity. It is made available under aCC-BY 4.0 International license.

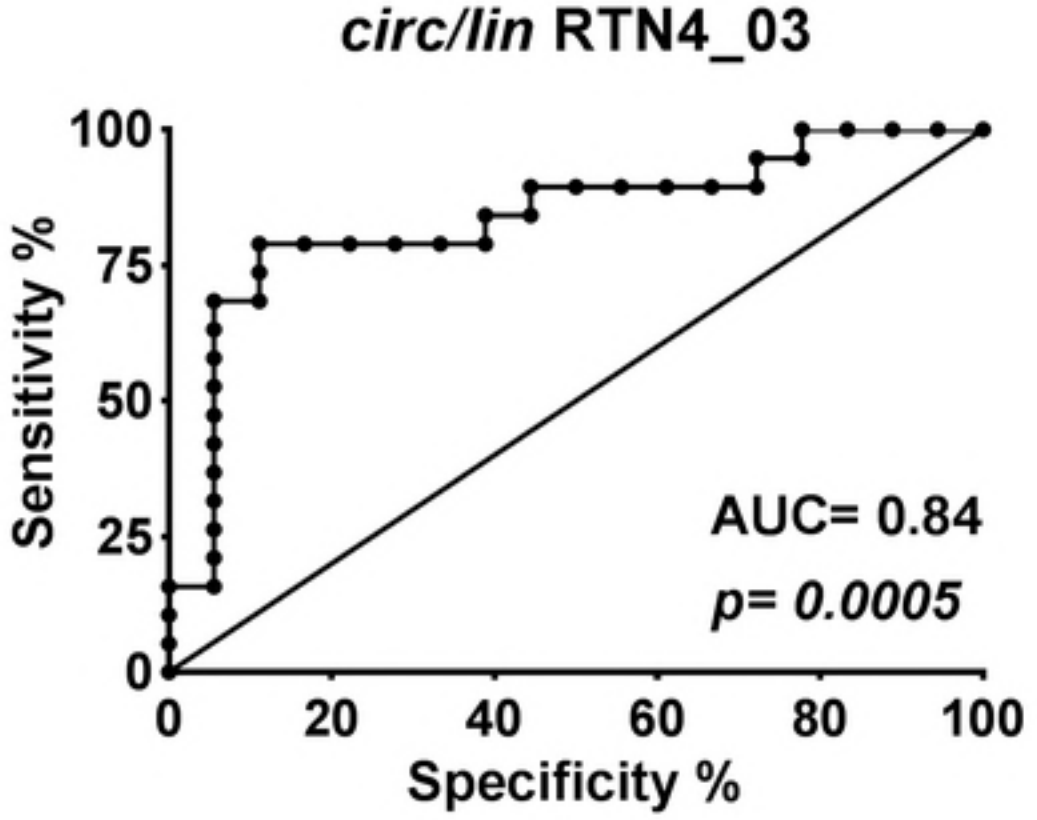

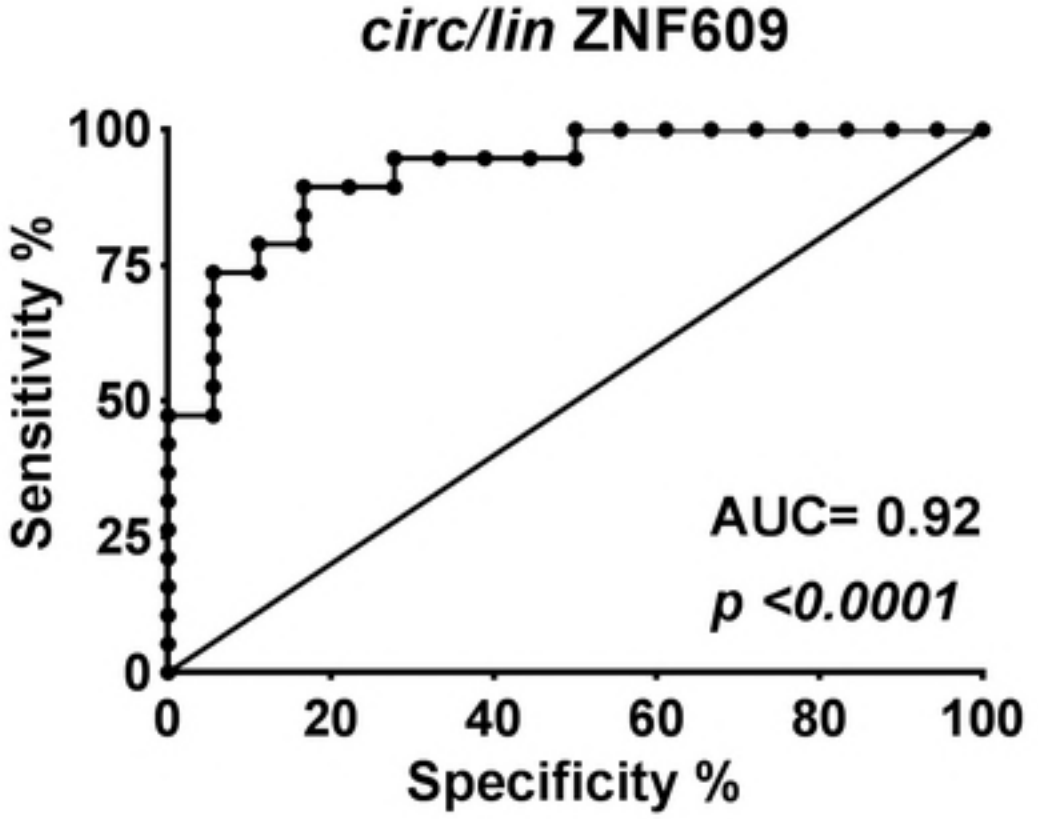

b

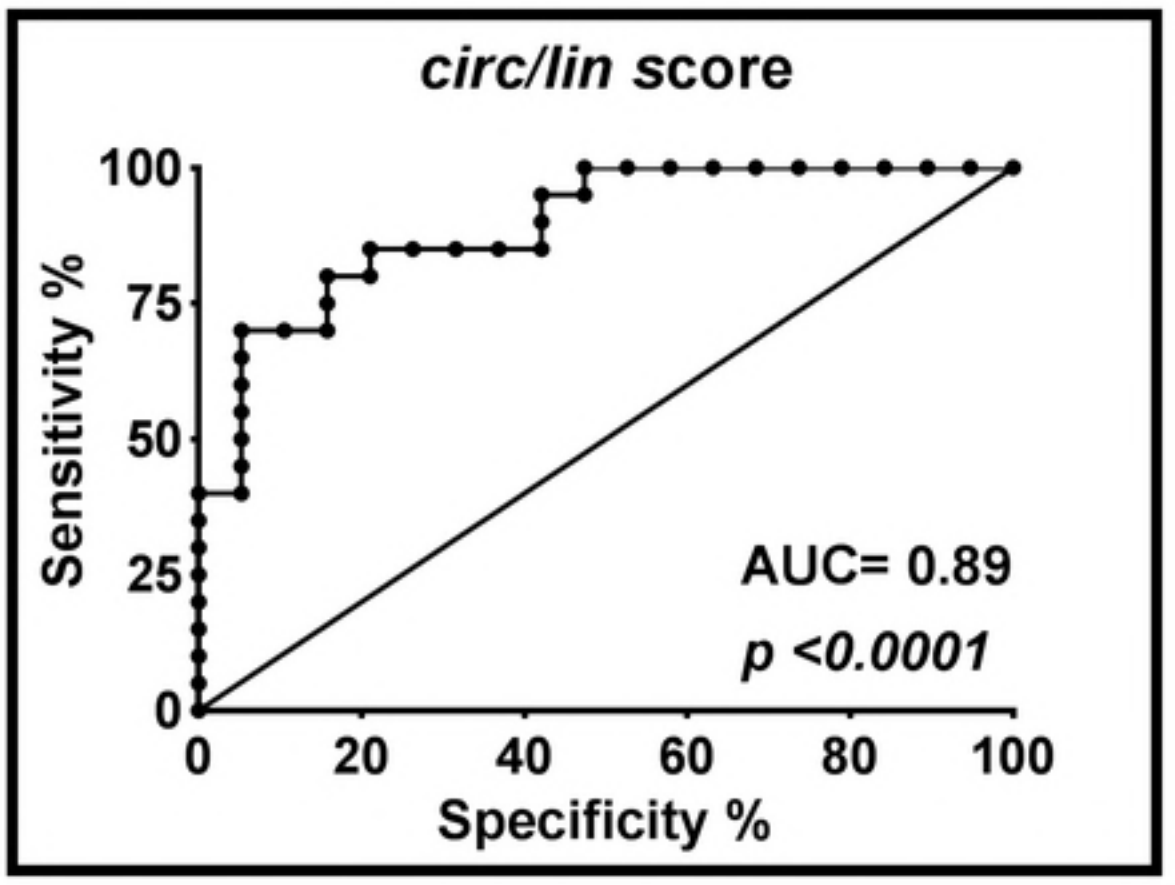

Figure2

a

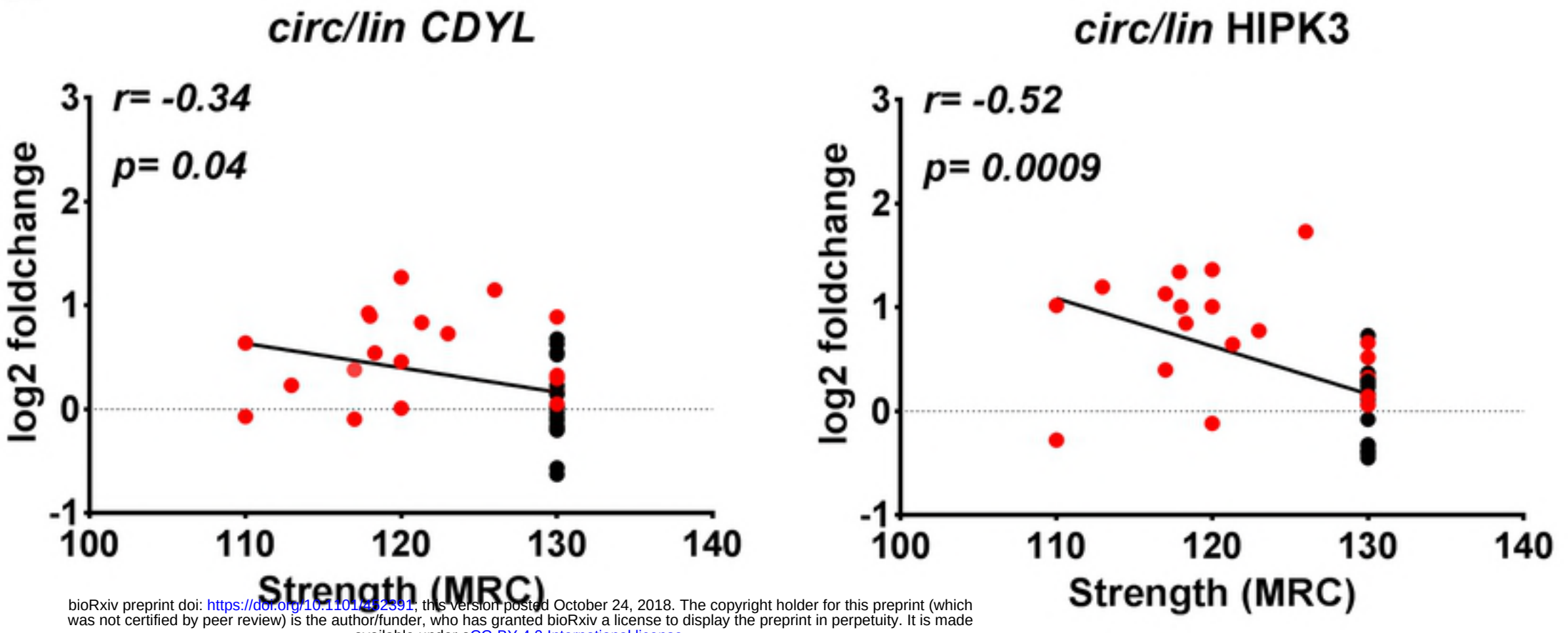

bioRxiv preprint doi: https://doi.org/10.1101/452391, this version posted October 24, 2018. The copyright holder for this preprint (which was not certified by peer review) is the author/funder, who has granted bioRxiv a license to display the preprint in perpetuity. It is made available under aCC-BY 4.0 International license.

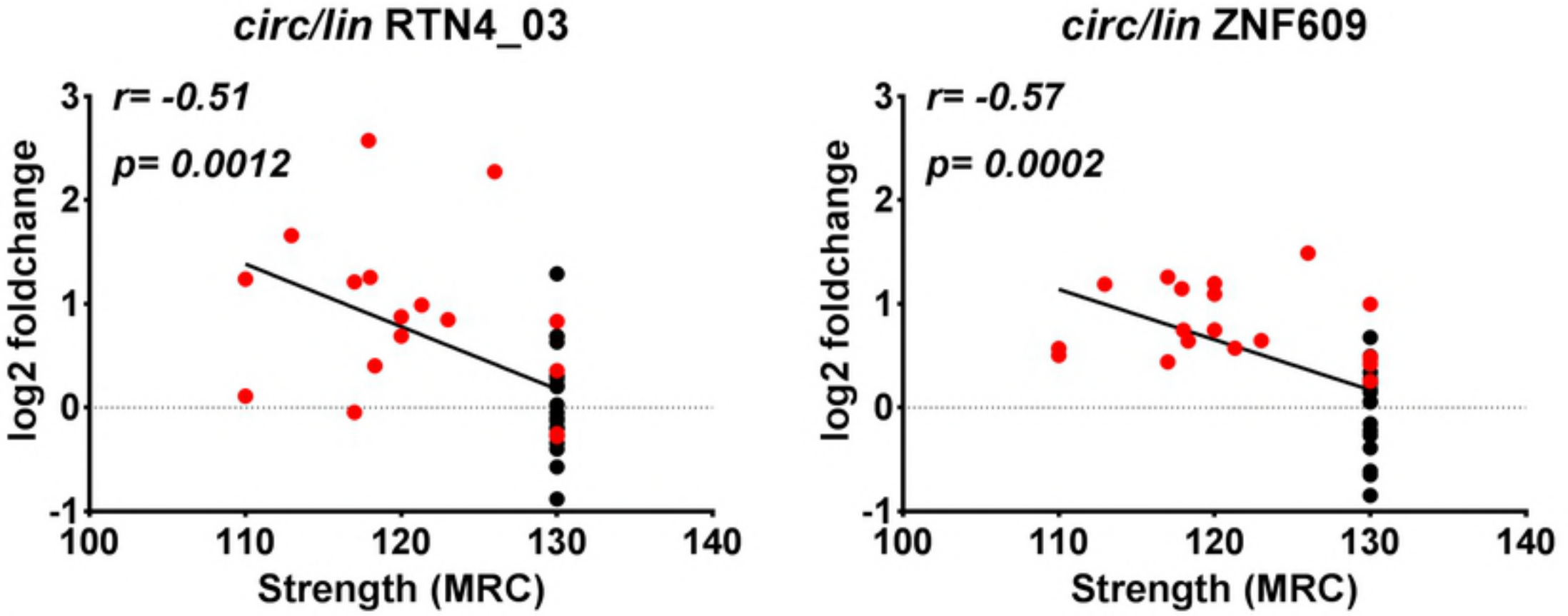

b

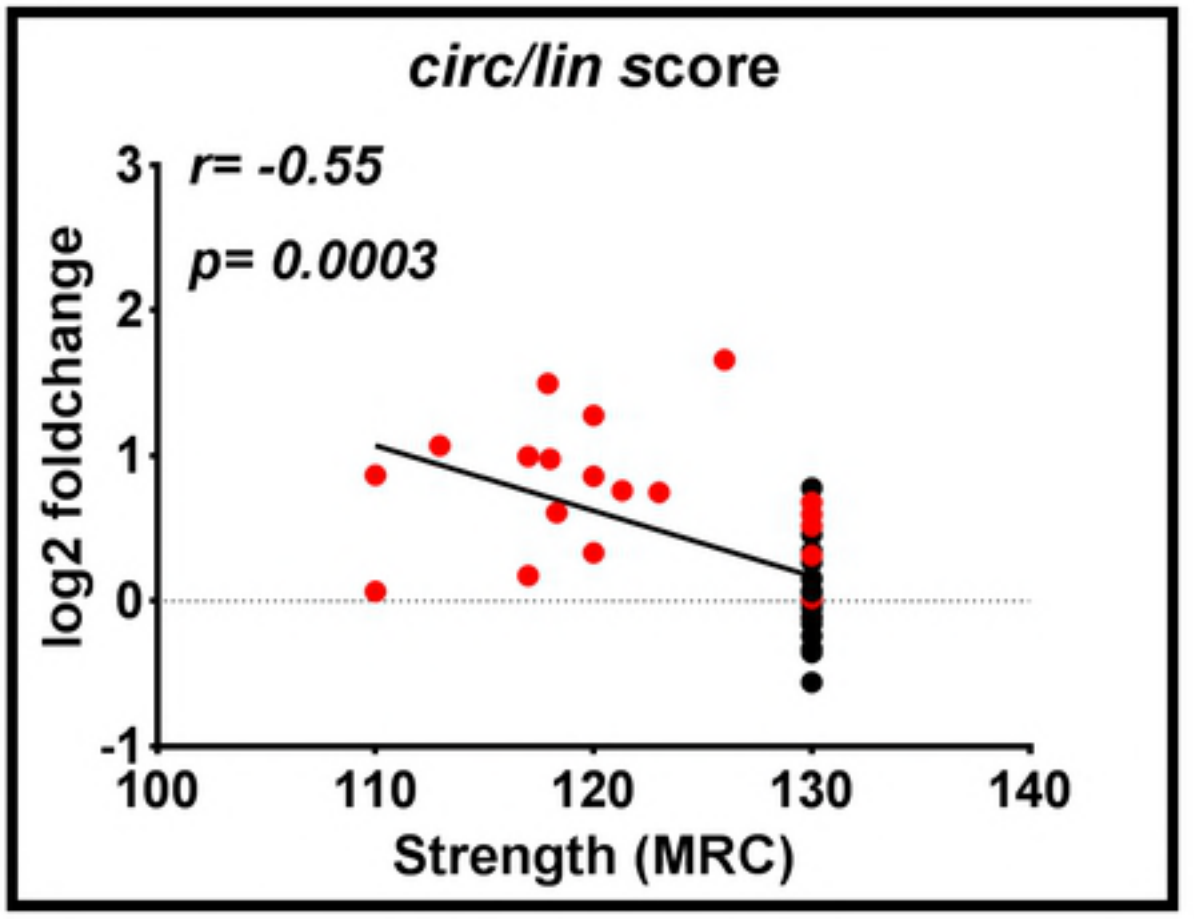

Figure3

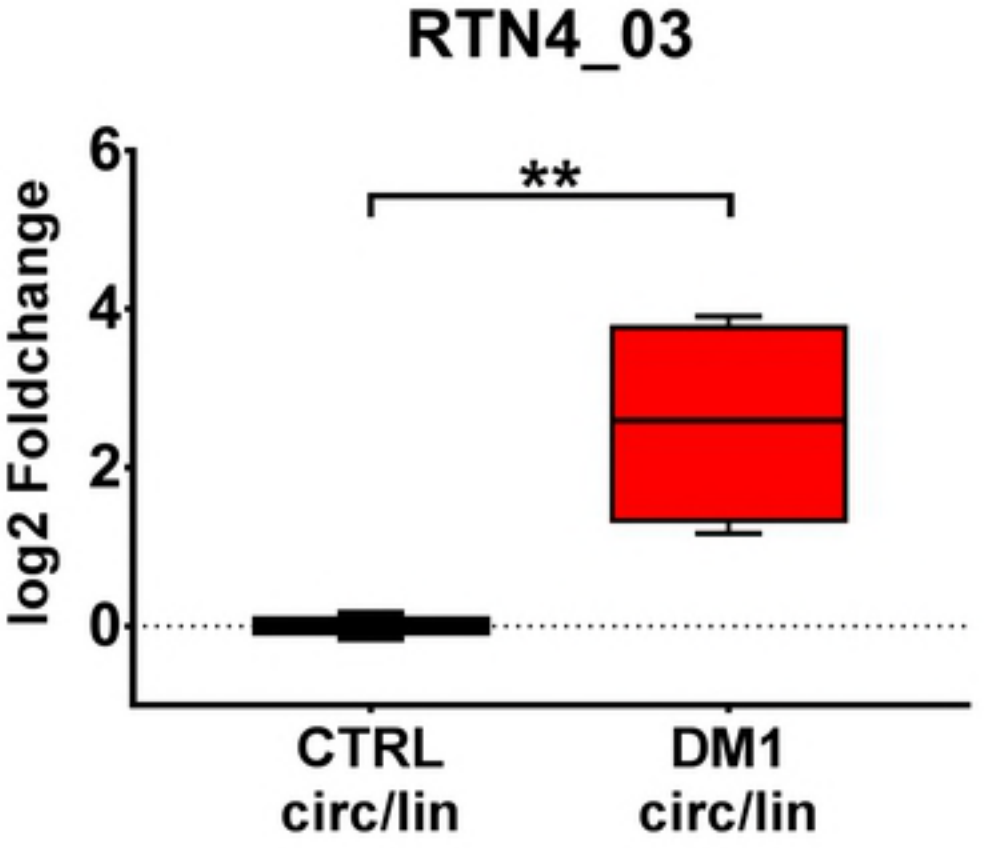
RTN4_03
log2 Foldchange
6
4
2
0
**
CTRL
circ/lin
DM1
circ/lin

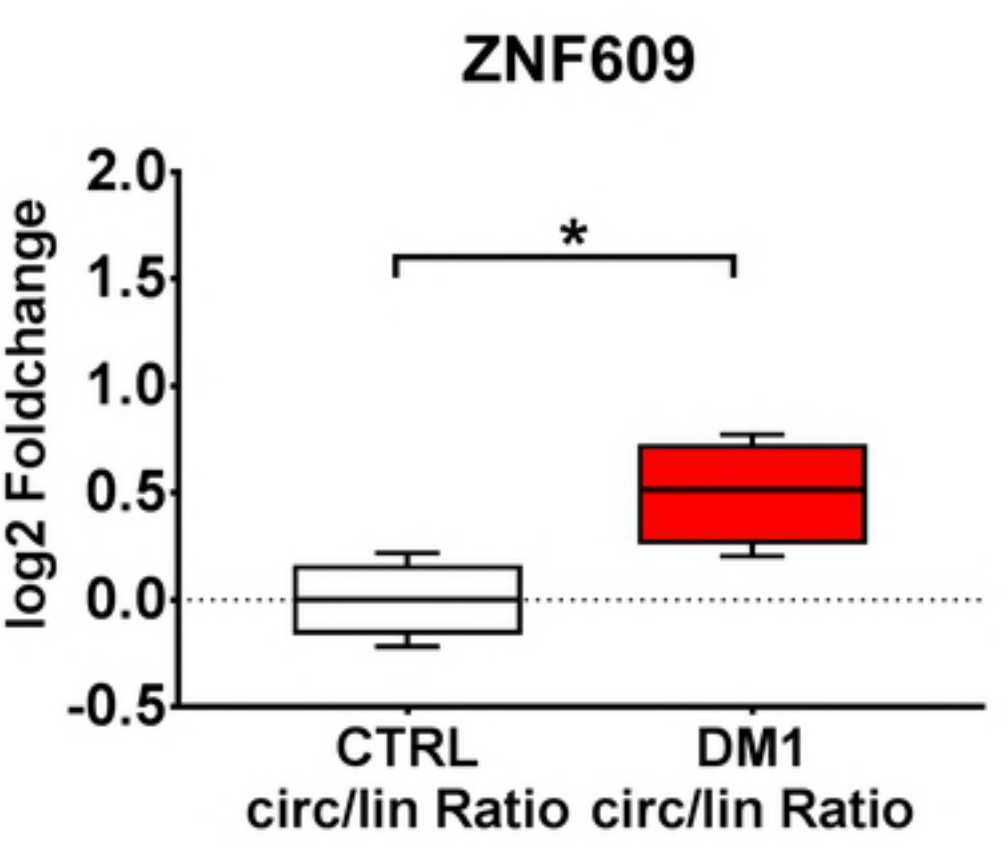
ZNF609
log2 Foldchange
2.0
1.5
1.0
0.5
0.0
-0.5
*
CTRL
circ/lin Ratio
DM1
circ/lin Ratio

Figure4

a

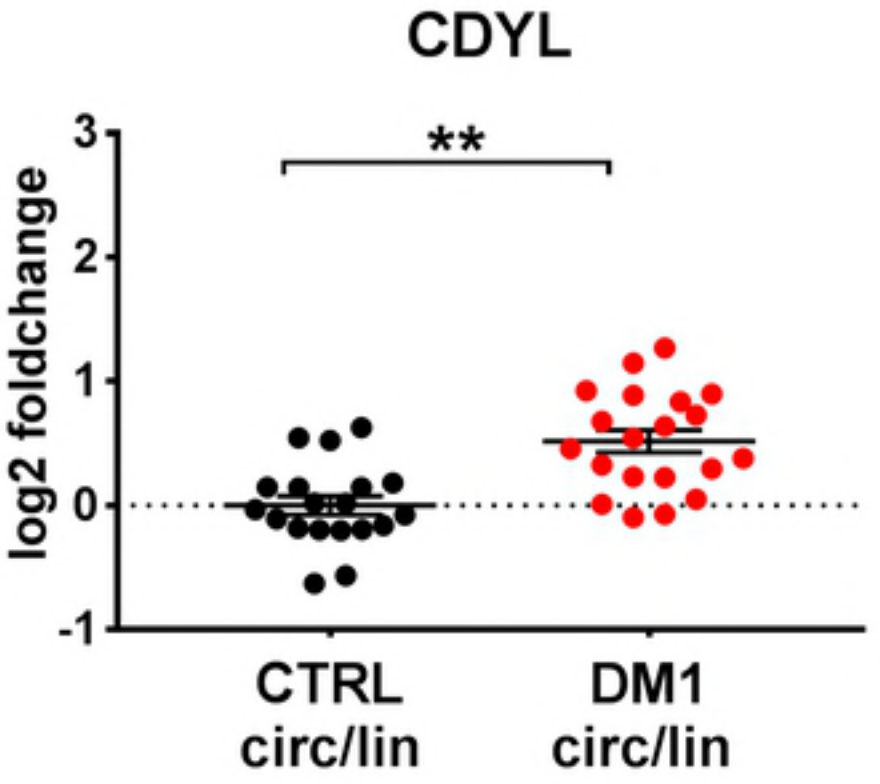

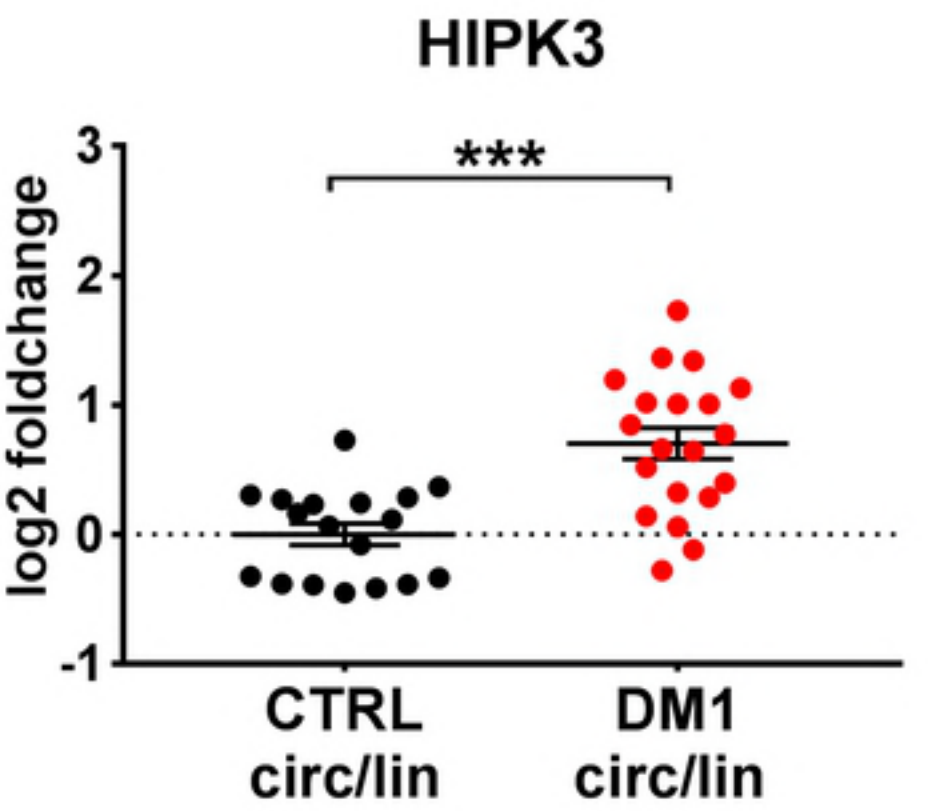

bioRxiv preprint doi: https://doi.org/10.1101/452391; this version posted October 24, 2018. The copyright holder for this preprint (which was not certified by peer review) is the author/funder, who has granted bioRxiv a license to display the preprint in perpetuity. It is made available under aCC-BY 4.0 International license.

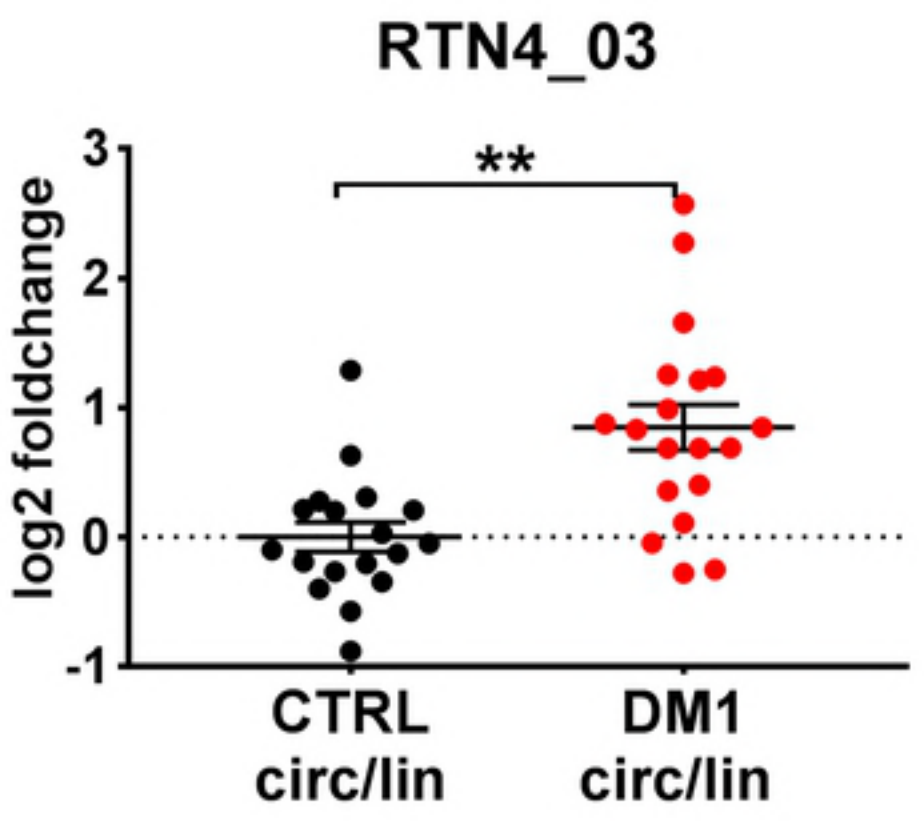

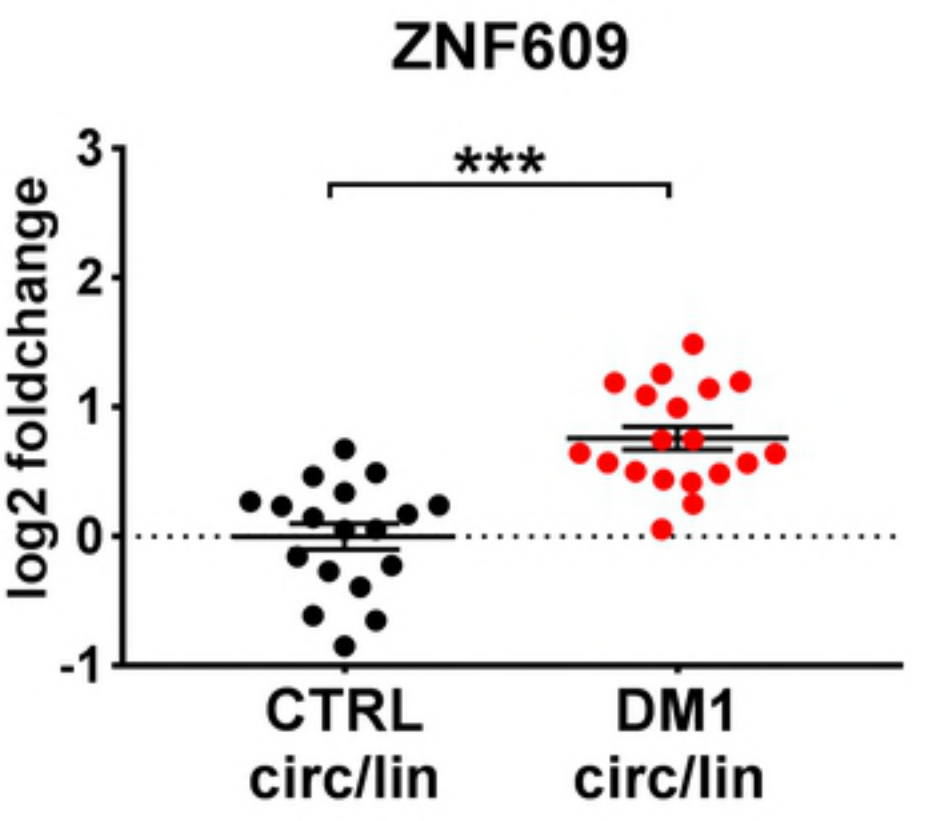

b

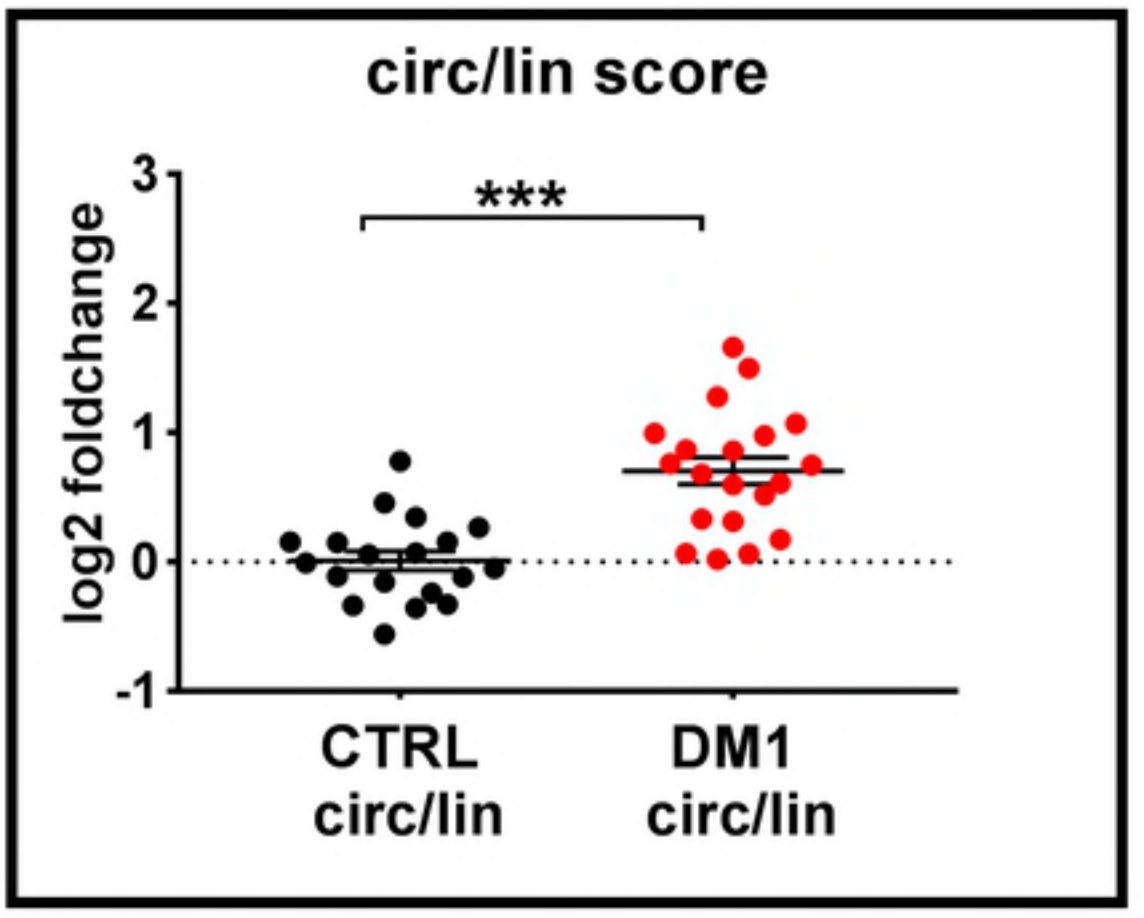

Figure1